

Design and Analysis of a High-Performance Capsule-Shaped 2D-Photonic Crystal Biosensor: Application in Biomedicine

H. Tayoub^{1,2,*}, A. Hocini^{1,†}, A. Harhouz^{1,‡}

¹ *Laboratoire d'Analyse des Signaux et Systèmes, Department of Electronics, University of M'Sila BP.166, Route Ichebilia, M'Sila, 28000, Algeria*

² *Research Center in Industrial Technologies CRTI, P.O.BOX:64, Cheraga 16014, Algiers-Algeria*

(Received 12 September 2021; revised manuscript received 02 December 2021; published online 20 December 2021)

In this paper, a novel capsule-shaped two-dimensional photonic crystal (2D-PhC) biosensor, which can sense different body fluids and cancer cells for biomedical applications, has been successfully proposed, designed, and evaluated. Simulation and analysis using Plane Wave Expansion (PWE) method and Finite-Difference Time-Domain (FDTD) algorithm have been done to detect blood components and cancer cells, in which samples are taken in liquid form and penetrate a capsule-shaped cavity. It consists of a capsule-shaped cavity coupled to two waveguides, and the sensing region has a capsular geometry and is positioned in the central region of the optical waveguide. The sensing mechanism of the present biosensor is based on changing the refractive index of the analyte. A high sensitivity of 609.25 nm per refractive index unit (nm/RIU), a low detection limit of 3.9×10^{-6} RIU and a Q-factor of up to 10^7 are predicted for a specific sensor-array arrangement in the wavelength range of 1.4367 to 2.0233 μm . These values demonstrate the potentiality of the proposed biosensor. To ensure the validity of the proposed biosensor, a comparison between the results of the present work and related literature for 2D-PhC biosensors has been made.

Keywords: PhC biosensor, Blood components, Cancer, Sensitivity, Quality-factor, Capsule-microcavity.

DOI: [10.21272/jnep.13\(6\).06005](https://doi.org/10.21272/jnep.13(6).06005)

PACS numbers: 07.07.Df, 42.79.Pw

1. INTRODUCTION

In recent years, the bio-related industry has developed rapidly due to its application in the detection and monitoring of various diseases. Due to the complexity of biomolecules and high-cost manufacturing processes, conventional techniques are not enough anymore. The detection, delivery and expression of biomolecules such as DNA, RNA and protein are essential for the prevention and treatment of diseases. Therefore, many nanotechnology-based methods and technologies have been developed to improve the detection sensitivity of these biomolecules, while simplifying and reducing the cost of the detection process. Among these nanomaterials is a Photonic Crystal (PhC) [1]. PhC materials have high sensitivity, high selectivity, and real-time monitoring capabilities, so they are attracting more and more attention in the fields of biochemistry and biomedicine. PhCs are composed of periodic lattices of dielectric materials. The periodicity gives them unique optical features, the creation of an optical bandgap is one of their most important specifications. Due to the photonic bandgap, PhCs can easily confine light. Leland C. Clark [2] demonstrated the first biosensor for the detection of glucose concentration in the blood in 1962. A PhC biosensor is a self-contained device, which can provide analytical information using biological recognition elements. Optical biosensors are especially employed for sensing several biological targets, such as cells, viruses, bacteria, hormones, proteins, enzymes, and nucleic acids. Several PhC biosensors have been proposed in the literature, in bio-sensing applications [3], breast cancer, and cancer cell detection [4]. Significant

reduction in the mortality rate by prognosis and diagnosis of different diseases at the earliest stage is the ultimate goal of this paper. Thus, the diseases investigated are the following.

– Hematologic diseases, disorders of the blood and blood-forming organs afflict millions of humans across the world. They cause many noncommunicable diseases (NCD), including cardiovascular disease, cancer, diabetes, and several hidden diseases, which bring 50 million deaths every year worldwide [5], that led to numerous studies for different blood component detection.

– Cancer is the principal cause of death in the world, it caused nearly 10 million deaths in 2020 [6]. Cancerous cells normally have larger refractive indices than normal cells [7], which makes them suitable to be used as an analyte in PhC sensors. N.R. Ramanujam [8] proposed a one-dimensional nanocomposite material-coated PhC sensor with a sensitivity of 43 nm/RIU. Another version of a 2D-PhC biosensor for the detection of cervical cancer cells was described by Hemanth Kumar B.M. et al. [9]. The sensitivity and the quality factor of the proposed biosensor are 143 nm/RIU and 248, respectively. The evolution of biosensors to detect basal cell carcinoma (BCC) was also investigated by Anna N. Yaroslavsky et al. [10], H. Chopra et al. [11], P. Sharma et al. [12], and Mohammad Danaie et al. [13]. Abdullah Al-Mamun Bulbul et al. [14] reviewed the application of a PCF-based biosensor in the THz regime for the detection of breast cancer cells.

– In this context, we propose a highly sensitive capsule-shaped 2D-PhC biosensor. The proposed PhC biosensor can be used simultaneously for detecting differ-

* hadjira.tayoub@univ-msila.dz

† abdesselam.hocini@univ-msila.dz

‡ ahlam.harhouz@univ-msila.dz

ent blood components and cancer cells by infiltrating the body fluid in a capsule-shaped microcavity. The proposed design maintains strong light-matter interaction in the capsule-shaped cavity, so a high sensitivity can be obtained. The proposed high-performance PhC biosensor can be used as a valuable diagnostic tool to detect diseases. The Plane Wave Expansion (PWE) method and the two-dimensional Finite-Difference Time-Domain (FDTD) algorithm simulations of the proposed biosensor have been carried out using RSoft Photonic Suite CAD FullWAVE and BandSOLVE simulator. Our designed biosensor is lightweight, ultra-small, and can be fabricated as a lab-on-chip sensor, which will make the detection of diseases much easier, more efficient, and inexpensive.

2. DESIGN OF PHOTONIC CRYSTAL BIOSENSOR

The proposed biosensor is made up of 2D triangular lattices, the size of the PhC structure is 39×23 . The lattice constant (a) is considered as $0.43 \mu\text{m}$, the air hole radius (r) is $0.14 \mu\text{m}$, where the refractive index profile of the Si slab $n_{\text{Si}} = 3.48$. The biosensor consists of two waveguides obtained by removing one row of air holes in the ΓK direction and a capsule-shaped cavity placed in the central zone of the biosensor on both sides to attain the highest output transmission. The radii of the three holes between the two waveguides and the microcavity are modified by changing their radius as follows: $R_1 = 0.41a$, $R_2 = 0.39a$, and $R_3 = 0.37a$ [15]. It is important to note that the infiltration is local in both capsules, where the capsules are totally injected with the analyte. 2D Plane Wave Expansion (2D-PWE) and FDTD were used to analyze the proposed biosensor.

3. RESULTS AND ANALYSIS

The photonic bandgap (PBG) of the designed PhC structure without any defects extends from $\omega_1 = 0.21252(a/\lambda)$ to $\omega_2 = 0.29929(a/\lambda)$ having a large bandgap in the wavelength range of $1.4367\text{-}2.0233 \mu\text{m}$ for a TM-polarized wave, which is calculated by the 2D-PWE method of BandSolve software.

It is widely known that the periodicity of the dielectric function of a PhC is broken if defects are introduced into its periodic lattice structure. Thus, the waveguide W1 obtained by omitting a row of air holes in the photonic lattice in the ΓK direction is shown in Fig. 1. This type of defect induces guided modes with frequencies in the PBG range [16].

The aim of using a capsule-shaped cavity with an enlarged size is to facilitate the infiltration process, enhance light-matter interaction, and reduce losses in the structure. As illustrated in Fig. 1a, the capsule-shaped cavity is positioned symmetrically in the central zone of the proposed biosensor, where the capsule length $L = a$ and the capsule radius $R = r$ (Fig. 1b).

Fig. 2a illustrates the normalized transmission spectrum of the proposed biosensor obtained using the FDTD method. We can clearly see a shift to higher values of the normalized transmission by increasing the refractive index.

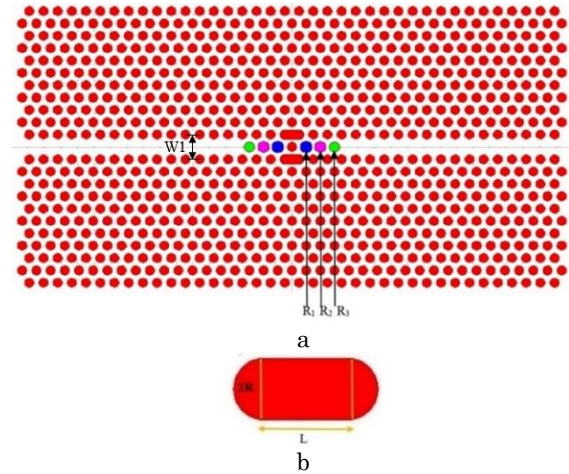


Fig. 1 – Schematic of the capsule-shaped 2D-PhC sensor (a), geometrical parameters of the capsule-shaped cavity, namely L and R (b)

Considering $n = 1$ as a reference, we achieved equivalent sensitivities for refractive indices $n = 1.1$, $n = 1.2$, $n = 1.3$ and $n = 1.4$ as follows: 515.9, 503.35, 485.73, and 465.47, respectively, and a high-quality factor (Q-factor) of up to 10^4 (Fig. 2b). We noticed that introducing the capsule-shaped cavity into the structure enhances the performance of the proposed sensor.

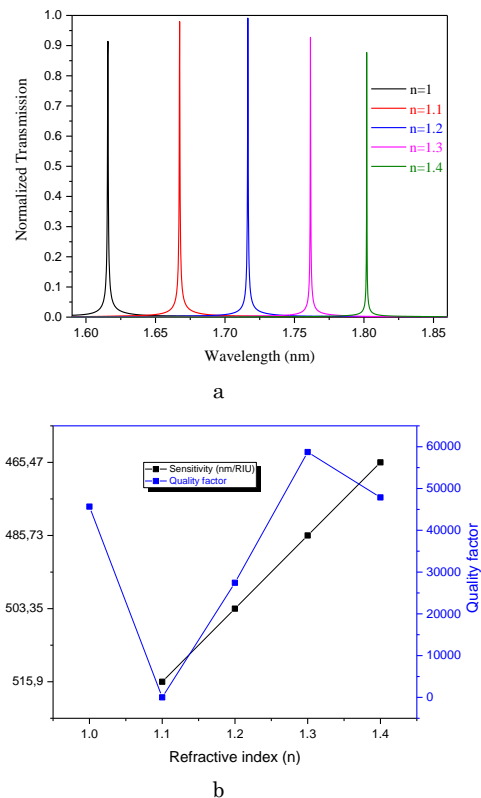


Fig. 2 – Normalized transmission spectrum of the PhC sensor for different refractive indices ranging from $n = 1$ to $n = 1.4$ with an increment of $\Delta n = 0.1$ (a), the calculated sensitivity and Q-factor of the proposed biosensor (b)

In this section, the proposed PhC biosensor will be used for the detection of different blood components, which were used as an analyte, and the normalized

transmission (Fig. 3), resonant wavelength, Q-factor, and sensitivity were observed (Table 1). Different blood constituents have different permittivity (ϵ), $\epsilon = n^2$, n is the refractive index, and as the permittivity of the bio-sample changes, there will be a change in the refractive index. According to the achieved results, with a small change in the refractive index, there will be a significant shift in the transmission for each blood constituent. The biosensor is highly sensitive and reported a sensitivity of 393 nm/RIU and a Q-factor of 3.8599×10^5 .

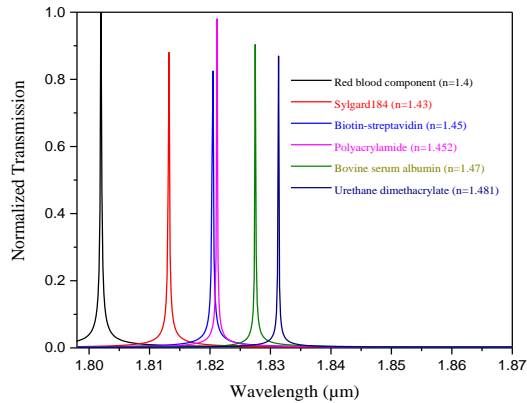


Fig. 3 – Normalized transmission spectrum achieved for different blood components

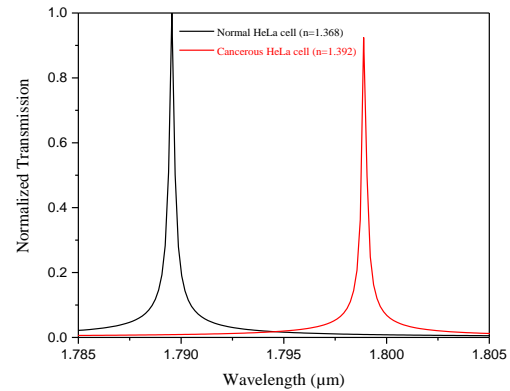
Another key feature of interest in this work is to differentiate between normal and cancer cell lines by infiltrating different sample cells in the capsule-shaped cavity. Here, we introduced both the cancerous cells and normal cells as an analyte in the capsule-shaped cavity. The proposed biosensor normalized transmission versus wavelength using the FDTD method is shown in Fig. 5. The transmittance peak of a normal cell is compared to that of a cancerous cell, and a shift to the right is observed for a cancerous cell. The wavelength shift depends on the refractive index of the sample and indicates the presence of cancerous cells.

Fig. 4a represents the resonant peak of 1.78955 μm for a normal HeLa cell ($n = 1.368$), which shifts to 1.79888 μm for a cancerous HeLa cell ($n = 1.392$). Fig. 4b represents the resonant peak of 1.78635 μm for a normal basal cell ($n = 1.36$), shifting to 1.79421 μm for a cancerous basal cell ($n = 1.38$). Fig. 4c shows the resonant peak of 1.79614 μm for a normal breast cell line ($n = 1.385$), which shifts to 1.80164 μm for a cancerous breast cell line ($n = 1.399$). The obtained sensitivities for a cancerous basal cell, a cancerous HeLa cell, and a cancerous breast cell are 393, 388.75 and 392.85 nm/RIU, respectively. They indicate that the proposed biosensor is highly sensitive to changes in the refractive index and, thus, can differentiate normal and cancerous cells.

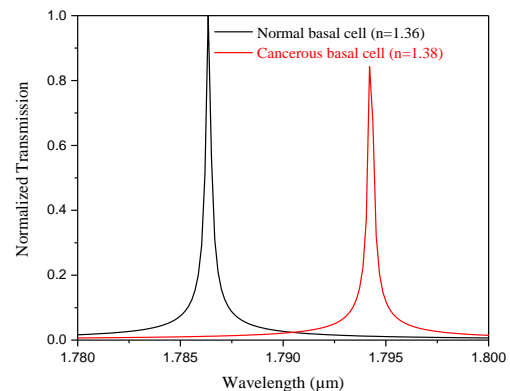
Our ultimate goal is to increase the performance of the capsule-shaped PhC biosensor. Further, more advanced biosensor designs are proposed.

The development of biosensor designs that increase sensitivity is extremely vital. Fig. 5 shows various proposed designs in order to realize high sensitivity; four designs were developed and analyzed. Specific design parameters were studied for optimal designs in terms of higher sensitivity. In Design A, the number of func-

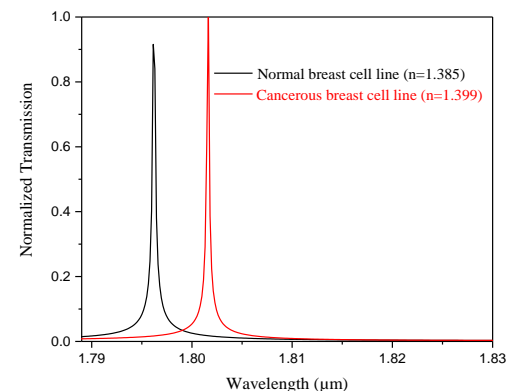
functionalized holes is increased (holes are colored yellow in Fig. 5), due to the fact that sensitivity is higher for a larger number of functionalized holes [17]. In Designs B, C, and D, two waveguides are placed at the bottom and top of the sensing area. A continuous wave is launched in the bottom waveguide, resonance occurs in the cavity, and the wave is transmitted from the bottom to the top waveguide. Finally, the wave leaves the top waveguide, and a time monitor is used at the output to get the transmission spectrum. A coupling distance of five rows between the waveguides and the capsule-shaped cavity was considered to achieve higher performance of the proposed biosensor. By increasing



a



b



c

Fig. 4 – Normalized transmission spectrum for normal and cancerous HeLa cell lines (a), basal cell lines (b), and breast cell lines (c)

coupling distance, the interaction of light with analyte

in the sensing area is reduced. Hence, by selecting five rows as the coupling distance, all features of the biosensor revealed suitable values. Indeed, as the length L of the capsule-shaped cavity increases, the sensitivity increases [18]; we suggest adding other capsules in

designs with larger lengths. The biosensor performance can be improved just by optimizing the number and length of capsule-shaped cavities and the number of functionalized holes.

Table 1 – Capsule-shaped biosensor performance for different analytes

	Wavelength (μm)	Q-factor	Sensitivity (nm/RIU)
Blood components			
Red blood component ($n = 1.4$)	1.80196	47864	Ref
Sylgard184 ($n = 1.43$)	1.81324	3.8599×10^5	376
Biotin-streptavidin ($n = 1.45$)	1.8205	24869	370.8
Polyacrylamide ($n = 1.452$)	1.82116	2.7095×10^5	369.23
Bovine serum albumin ($n = 1.47$)	1.82749	22035	364.71
Urethane dimethacrylate ($n = 1.481$)	1.83133	23029	362.59
Cancer cells			
Normal basal cell ($n = 1.36$)	1.78635	68729	Ref
Cancerous basal cell ($n = 1.38$)	1.79421	20475	393
Normal HeLa cell ($n = 1.368$)	1.78955	85547	Ref
Cancerous HeLa cell ($n = 1.392$)	1.79888	46894	388.75
Normal breast cell line ($n = 1.385$)	1.79614	37099	Ref
Cancerous breast cell line ($n = 1.399$)	1.80164	13774	392.85

Table 2 – Comparison of the proposed biosensor with prior PhC biosensors

References	Sensitivity (nm/RIU)	Q-factor	Detection limit (RIU)	Sensing parameters	Year
[19]	—	262	0.002	Blood components	2018
[8]	43	—	—	Cancer cell	2018
[11]	6.6525	1094.76	—	Cancer cell	2016
	5.95	1110.48		Blood components	
This work					
Design A	460.33	1.032×10^7	3.902×10^{-6}	Blood components/ Cancer cell/	—
Design B	573	60276	5.53×10^{-6}		
Design C	587	67771	4.65×10^{-6}		
Design D	609.25	42708	6.51×10^{-6}		

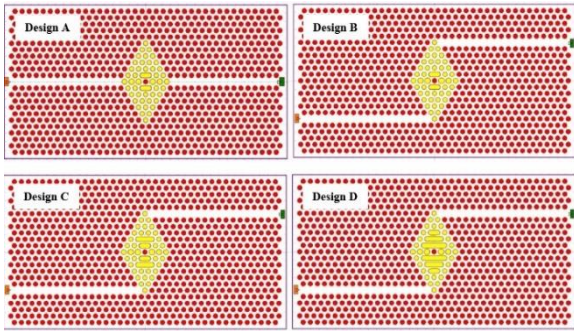
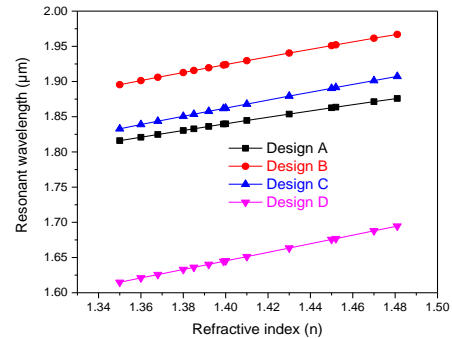


Fig. 5 – Different designs in which capsule-shaped cavities are infiltrated with the analyte as well as the holes in yellow color. **Design A** and **Design B**: the capsule length $L = a$ and the capsule radius $R = r$; **Design C**: the 1st capsule with $L = a$ and $R = r$ and the 2nd capsule with $L = 2a$ and $R = r$; **Design D**: the 1st capsule with $L = 3a$ and $R = r$, the 2nd capsule with $L = 2a$ and $R = r$, and the 3rd capsule with $L = a$ and $R = r$

The main results of the proposed designs are summarized in Fig. 6. As illustrated in Fig. 6a, the resonant wavelength of the biosensor shifts linearly towards higher wavelengths with increasing refractive index, it is extremely sensitive to a small change in the refractive index and simultaneously the sensitivity

increases. It is noticed that with an increase in the number of capsule-shaped cavities, there is a favorable increase in sensitivity (see Fig. 6b) due to the significant influence of the holes around the capsule-shaped cavity, the sensitivity increases to the highest value of $S = 609.25$ nm/RIU.

Table 2 shows a comparison of the performance of the proposed biosensor with other related biosensors reported in the last five years. The results indicate that the proposed biosensor has high sensitivity, extremely high Q-factor, and very low detection limit.



a

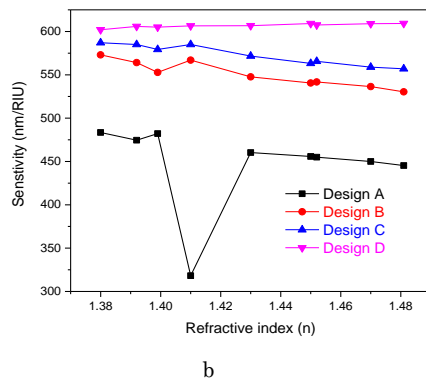


Fig. 6 – Resonant wavelength variations depending on changes in the refractive index for four designs (a), the calculated sensitivity of the proposed four designs (b)

REFERENCES

1. C. Fenzl, T. Hirsch, O.S. Wolfbeis, *Angew. Chemie – Int. Ed.* **53**, 3318 (2014).
2. L. Clark Jr, *Implantable Gas-Containing Biosensor and Method for Measuring an Analyte Such as Glucose*, US patent 4,680,268.
3. S. Olyaei, A. Mohebzadeh-Bahabady, *Opt. Quantum Electron.* **47**, 1881 (2015).
4. P. Sharan, S.M. Bharadwaj, F.D. Gudagunti, P. Deshmukh, *2014 Int. Conf. IMPACT E-Technology US, IMPETUS*, 20 (2014).
5. P. Sharma, P. Sharan, *Opt. Commun.* **348**, 19 (2015).
6. J. Ferlay, M. Ervik, F. Lam, M. Colombet, L. Mery, M. Piñeros, *Global Cancer Observatory: Cancer Today*.
7. S. Jindal, S. Sobti, M. Kumar, S. Sharma, M.K. Pal, *IEEE Sens. J.* **16**, 3705 (2016).
8. N.R. Ramanujam, I.S. Amiri, S.A. Taya, S. Olyaei, R. Udaiyakumar, A. Pasumpon Pandian, K.S. Joseph Wilson, P. Mahalakshmi, P.P. Ypapin, *Microsyst. Technol.* **25**, 189 (2019).
9. B.M.H. Kumar, A.M. Vaibar, P.C. Srikanth, *Proc. CONECT 2020 - 6th IEEE Int. Conf. Electron. Comput. Commun. Technol.* 1 (2020).
10. A.N. Yaroslavsky, R. Patel, E. Salomatina, C. Li, C. Lin, M. Al-Arashi, V. Neel, *Opt. Lett.* **37**, 644 (2012).
11. H. Chopra, R.S. Kaler, B. Painam, *J. Nanophoton.* **10**, 036011 (2016).
12. P. Sharma, P. Sharan, P. Deshmukh, *2015 Int. Conf. Pervasive Comput. Adv. Commun. Technol. Appl. Soc. ICPC 2* (2015).
13. D. Mohammad, K. Behnam, *Photon. Nanostruct. – Fundam. Appl.* **31**, 89 (2018).
14. A.A.M. Bulbul, H. Rahaman, S. Biswas, M.B. Hossain, A. Al Nahid, *Sens. Bio-Sensing Res.* **30**, 100388 (2020).
15. M. Ammari, F. Hobar, M. Bouchemat, *Chinese J. Phys.* **56**, 1415 (2018).
16. Y. Zhao, C. Qian, K. Qiu, Y. Gao, X. Xu, *Opt. Exp.* **23**, 9211 (2016).
17. Y.N. Zhang, Y. Zhao, Q. Wang, *Sensor. Actuat. B: Chem.* **209**, 431 (2015).
18. M. Maache, Y. Fazea, A.A. Alkahtani, I.U. Din, *Symmetry (Basel)* **12**, 1480 (2020).
19. R. Arunkumar, T. Suaganya, S. Robinson, *Photon. Sensor.* **9**, 69 (2019).

Розробка та аналіз високопродуктивного капсулоподібного біосенсора на 2D фотонних кристалах: застосування в біомедицині

Н. Tayoub^{1,2}, А. Hocini¹, А. Harhouz¹

¹ *Laboratoire d'Analyse des Signaux et Systèmes, Department of Electronics, University of M'Sila BP.166, Route Ichebilia, M'Sila, 28000, Algeria*

² *Research Center in Industrial Technologies CRTI, P.O.BOX:64, Cheraga 16014, Algiers-Algeria*

У статті успішно запропонований, розроблений та оцінений новий капсулоподібний біосенсор на двовимірних фотонних кристалах (2D-PhC), який може визначати різні рідини організму та ракові клітини для біомедичних застосувань. Для виявлення компонентів крові та ракових клітин проведено моделювання та аналіз з використанням методу розкладання плоскої хвилі (PWE) та алгоритму кінцевих різниць у часовій області (FDTD), для яких відбираються зразки у рідкій формі та поміщуються у капсулоподібну порожнину. Біосенсор складається з капсулоподібної порожнини, з'єднаної з двома хвилеводами, а чутлива область має капсульну геометрію і розташована в центральній області оптичного хвилеводу. Чутливий механізм запропонованого біосенсора заснований на зміні показника заломлення аналіту. Висока чутливість 609,25 нм на одиницю показника заломлення (нм/RIU), низька межа виявлення $3,9 \times 10^{-6}$ RIU і добротність до 10^7 спрогнозовані для конкретного розташування сен-

сорної матриці в діапазоні довжин хвиль від 1,4367 до 2,0233 мкм. Ці значення демонструють потенціал біосенсора, який розглядається. Щоб переконатися у достовірності запропонованого біосенсора, проведено порівняння результатів цієї роботи та відповідної літератури для фотонно-кристалічних (2D-PhC) біосенсорів.

Ключові слова: Фотонно-кристалічний (PhC) біосенсор, Компоненти крові, Рак, Чутливість, Добротність, Капсула-мікропорожнина.